PROCEEDINGS OF SCIENCE

Vela-X as main contributor to the electron and positron spectra for energy above 100 GeV

D. Rozza[*ab], **S. Della Torre**[a], **M. Gervasi**[ab], **P.G. Rancoita**[a] **and A. Treves**[ac]
[a] *INFN Milano Bicocca*
Piazza della Scienza 3, 20126 Milano - Italy
[b] *University of Milano Bicocca*
Piazza Ateneo Nuovo 3, 20126 Milano - Italy
[c] *University of Insubria*
Via Valleggio 11, 22100 Como - Italy
E-mail: davide.rozza@mib.infn.it

The precise measurements of the electron plus positron spectra, in the energy range from 0.5 GeV up to 1 TeV, were published by the AMS-02 collaboration. We focus the attention above 10 GeV where the solar modulation effects are negligible. The differences between these data and the "classical" Local Interstellar Spectra, obtained using optimized GALPROP parameters, show an extra contribution suggesting an equal amount for both electrons and positrons. Thus, they would be generated by a pair production process from the same source. We studied the contribution from Pulsar Wind Nebulae starting from the photon spectrum (due to synchrotron and inverse Compton processes) detected by gamma-ray telescopes. A diffusion model is applied from the source up to the Solar System and the propagated spectra are compared with the AMS-02 data. Above 100 GeV, Vela-X is the main candidate to contribute to the observed excess, while, below 100 GeV, more aged pulsars like Monogem give a higher contribution. An estimation on the degree of anisotropy from these sources is also presented.

The 34th International Cosmic Ray Conference,
30 July- 6 August, 2015
The Hague, The Netherlands

*Speaker.

© Copyright owned by the author(s) under the terms of the Creative Commons Attribution-NonCommercial-ShareAlike Licence.

PoS(ICRC2015)501

1. Introduction

Electrons and positrons represent only $\sim 1\%$ of the galactic cosmic rays (CR) which reach the Earth. The standard description is that electrons are mainly produced and accelerated by supernova remnants, while positrons are supposed to be mainly originated from the decay of muons created in interactions between primary CR and the interstellar medium (ISM). Before reaching the Earth, CR electrons and positrons propagate in the Galaxy interacting with the ISM, magnetic and radiation fields. Nevertheless the "classical" scenario is not able to reproduce experimental data above ~ 10 GeV (specially in the positron spectrum). Indeed, the space born experiment AMS-02 measured with unprecedented precision electron and positron fluxes and pointed out a deviation from these predictions. In this work, we investigated possible astrophysical sources (i.e., pulsar wind nebulae - PWN) of positrons and electrons, which may account for the flux excess.

2. The model

2.1 The "classical" LIS

The CRs propagation in the Galaxy is described by equation (see e.g., [1, Chap. 3]):

$$\frac{\partial n_i}{\partial t} = Q_i + \vec{\nabla} \cdot \left[D_i \vec{\nabla} n_i \right] + \frac{\partial}{\partial E} \left[b_i n_i \right] - p_i n_i + P_i, \tag{2.1}$$

where the time evolution of the energy density $n_i = dN_i/dE$ of cosmic ray species i with energy E depends on the source term Q_i, diffusion coefficient D_i, the change of the particle energy per unit time b_i, catastrophic processes p_i and nuclei collisions P_i.

We used the GALPROP model to evaluate the local interstellar spectrum (LIS) and we tuned its parameters according to the experimental data reported in the cosmic ray database [2]. The GALPROP code[1] numerically solves equation (2.1) for different CR species in a cylindrically symmetric space [3] and returns the LIS for the specific particle at the Solar System. The solution of equation (2.1) depends on parameters like the boundary conditions of the galactic effective volume, the diffusion coefficient and the injection spectra characterized by power laws with different spectral indices for nuclei, protons and primary electrons. To set these parameters, we compared the so obtained LIS's with the experimental data above $\sim$10 GeV (where the solar modulation effects are negligible). We used a Galactic radius of 30 kpc, height ± 4 kpc and a diffusion coefficient depending on the energy as $D(E) = 5.8 \cdot 10^{28} [\mathrm{cm}^2 \mathrm{s}^{-1}] (E[\mathrm{GeV}]/4)^{0.33}$. Above 10 GeV, the injection spectral index for protons $\gamma_p = 2.42$, while for electrons $\gamma_e = 2.68$.

The GALPROP source term for electrons and positrons kept into account primary electrons produced and accelerated in supernova remnants (whose injection is described by γ_e), as well as secondary electrons and positrons produced in interactions between primary CRs and the ISM [4, 5]. Hereafter, we will refer to these GALPROP LIS as the "classical" electron and positron LIS's (cLIS). The electron plus positron cLIS, obtained with the GALPROP parameters reported above, is shown in figure 1. The cLIS is drawn in the energy range under analysis, above 10 GeV. An estimation of the uncertainty related to the propagation parameters leads to a deviation

[1] http://galprop.stanford.edu/webrun.php (2014)

PoS(ICRC2015)501

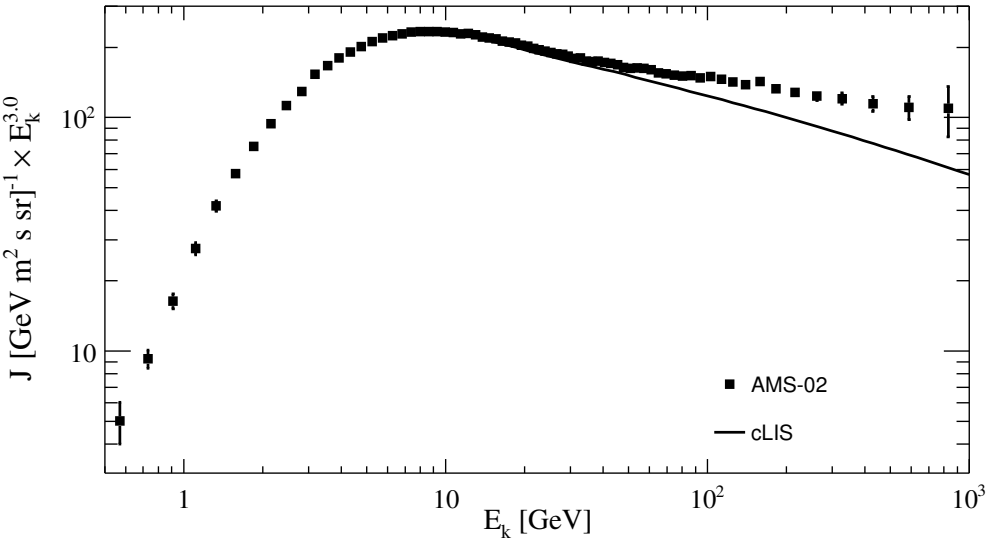

Figure 1: Electron plus positron cLIS compared with the AMS-02 spectrum.

of $\sim$ 15% at 1 TeV, decreases to 2% at 30 GeV and increases again at 15% at 10 GeV [6]. The comparison with the AMS-02 flux [7], reported in figure 1, shows an excess in the data of 10% at 50 GeV which increases at higher energies. We also compared the cLIS, obtained using the GALPROP parameters reported above, with electron and positron flux [8]. We got an excess amount for both electrons and positrons described by the same power law (same normalization and same slope) [6]. For these reason, sources of electron-positron pairs are needed to fill the gap shown in figure 1.

2.2 The PWN contribution

Pulsar wind nebulae are widely believed to be responsible for the acceleration of cosmic rays up to energies of 10^{15} eV [9, 10, 11]. These objects identify the region around the pulsars where a relativistic magnetized wind is populated with electron and positron pairs [12, 13] and they are characterised by a very wide photon spectrum supposed to be produced by these particles via synchrotron and inverse Compton processes.

Electrons and positrons are characterised by an high energy loss rate during their travel in the interstellar medium; we evaluated that an electron (or positron) with an initial energy of 100 GeV can travel at most for $\sim$ 2 kpc. Thus, sources of electron-positron pairs must be characterised by a distance less than 2 kpc from the Solar System. The TeVCat catalogue[2] contains less than 40 PWN's characterised by a photon spectrum that reaches the TeV region. Only five of them are closer than 2 kpc, but it is widely believed that PWN's are not more observable after the early phase of expansion (usually about 10^3-10^4 years [14]).

Among these sources, the most studied object is the Crab Nebula, the remnant of a supernova explosion observed in the year 1054. Cherenkov telescope experiments (see e.g., HESS [15] and Magic [16]) provide a complete and accurate description of the Crab spectral energy distribution.

[2]http://tevcat.uchicago.edu/ (2015)

PoS(ICRC2015)501

Together with parameters like the age, the rotational frequency and its derivatives, the Crab photon spectrum can be described as in [17, 18, 19]. Since we do not have enough information related to the rotational parameters or the gamma-ray emission of the other sources, the Crab object can be taken as a reference sample of the first phase of the life for a generic PSR/PWN.

To evaluate the energy spectrum of electrons and positrons at the source, we follow the approach reported in [17]. We used an electron injection rate described by a broken power law with indices α_1 and α_2 before and after an energy break E_b.

$$Q(E_e,t) = \begin{cases} Q_0(t)(E_e/E_b)^{\alpha_1} & \text{if } E_e < E_b, \\ Q_0(t)(E_e/E_b)^{\alpha_2} & \text{if } E_e > E_b, \end{cases} \tag{2.2}$$

where E_e is the particle kinetic energy and $Q_0(t)$ can be derived by requiring the continuity of the two power law and by the following condition:

$$\int_{E_{min}}^{E_{max}} Q(E_e,t) E_e dE_e = \eta L_{sd}(t), \tag{2.3}$$

with η the conversion factor of the spin-down power $L_{sd}(t)$ into particle luminosity. The particle spectrum over time from $t = 0$ to $t = T$ (age of the PWN) is:

$$\frac{dN(E_e,T)}{dE_e} = \int_0^T Q(E_e,t) \exp\left(-\frac{T-t}{\tau_{eff}}\right) dt; \tag{2.4}$$

where $\tau_{eff}^{-1} = \tau_{syn}^{-1} + \tau_{esc}^{-1}$ corresponds to the lifetime of an electron with respect to both synchrotron energy loss and escape timescale (i.e., the time to diffuse up to 1 PWN radius). Using the same parameters reported in Table 1 of [17], we reproduced the Crab photon spectrum. Assuming that all the pulsars reported in the second FERMI catalogue [20] are Crab-like at 1000 years, we have propagated the electron and positron spectrum (responsible of the PWN photon spectrum) up to Earth using the analytic solution of the equation (2.1) for this kind of particle [1, 14]:

$$\begin{aligned} J(\vec{x},E,t) &= \frac{\beta c}{4\pi} n_e(\vec{x},E,t) \\ &= \frac{\beta c}{4\pi} \frac{Q_0}{(4\pi\lambda_d^2)^{3/2}} E^{-\alpha} (1-b_0 t E)^{\alpha-2} \\ &\quad \times \exp\left[-\frac{E}{E_{cut}(1-b_0 t E)}\right] \exp\left(-\frac{|\vec{x}|^2}{4\lambda_d^2}\right), \end{aligned} \tag{2.5}$$

where λ_d is the mean distance travelled by particles with initial energy $E_0 = E/(1-b_0 t E)$ down to energy E resulting from both energy loss $dE/dt = -b(E) \sim -b_0 E^2 = 7 \cdot 10^{-17}$ GeV^{-1}s^{-1} E^2 and diffusion processes. The injection spectrum and all the other parameters were taken by the Crab model at 1000 years. The only differences were the distance and the age of the different FERMI objects. The main contribution above 100 GeV comes from Vela-X, while, below this energy, the contribution of Monogem is dominant. We also found that the contribution of all the other known pulsars is negligible. In figure 2, we report the Vela-X and Monogem contribution (taking into account both electrons and positrons) added to the cLIS presented in section 2.1. In figure 2 we show a comparison between our model and the AMS-02 data in the energy range between 10 GeV and 1 TeV.

PoS(ICRC2015)501

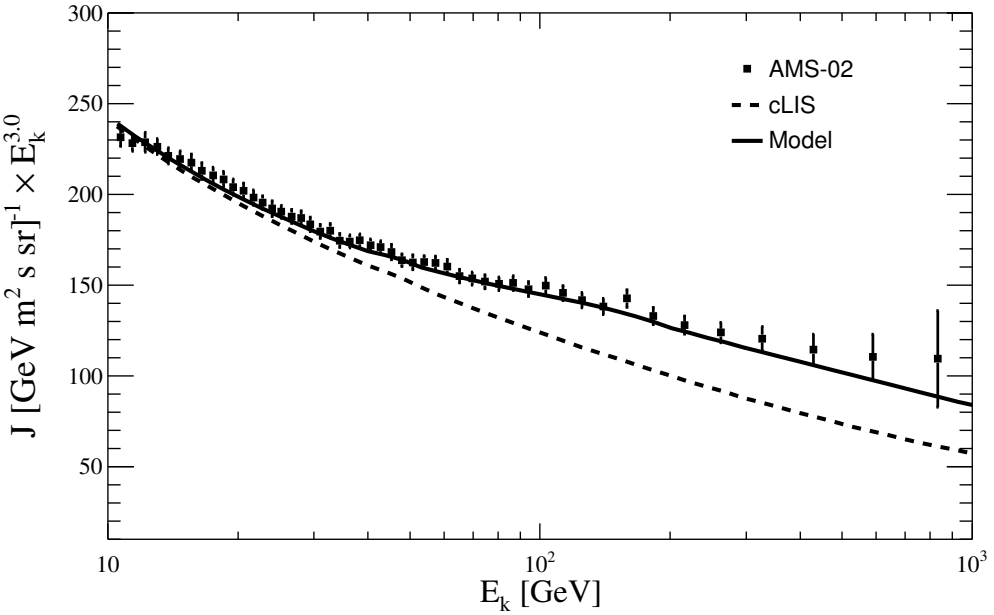

Figure 2: Our model for electron plus positron contribution coming from cLIS (dashed line) and from the sum of the cLIS, Vela-X and Monogem (solid line) compared with the AMS-02 data.

3. Anisotropy

As pointed out in section 2.2, two pulsar wind nebulae, Vela-X and Monogem, may be responsible for the electron and positron excess in CRs in comparison with cLIS models. Considering point-like sources, a dipole signal, directed along the line of sight of the source, in the CR could be detected. In this section, we evaluate the degree of anisotropy from single source.

The anisotropy of CRs coming from a point source, under the common assumption that the particle propagation in the Galaxy is usually described under the diffusion approximation, is described by [21, 22]. The degree of cosmic ray anisotropy from a single source is defined as:

$$\delta = \frac{I_{max} - I_{min}}{I_{max} + I_{min}}, \tag{3.1}$$

where I is the particle intensity depending on the direction. Assuming an isotropic diffusion of CR coming from a point source we get the sum of an isotropic signal of constant intensity I_0 and of a dipole anisotropy of maximum intensity I_1, the overall intensity at an angular distance ϑ from the maximum of the dipole anisotropy will be: $I(\vartheta) = I_0 + I_1 \cos\vartheta$. In this case, $I_{max} = I_0 + I_1$ is found looking at the direction of the source, while $I_{min} = I_0 - I_1$ is found in the opposite direction. The degree of the dipole anisotropy then becomes:

$$\delta = \frac{I_1}{I_0}. \tag{3.2}$$

The particle flux is defined integrating the intensity as following:

$$F = \int I(\vartheta)\cos\vartheta d\Omega = \frac{4\pi}{3} I_1. \tag{3.3}$$

PoS(ICRC2015)501

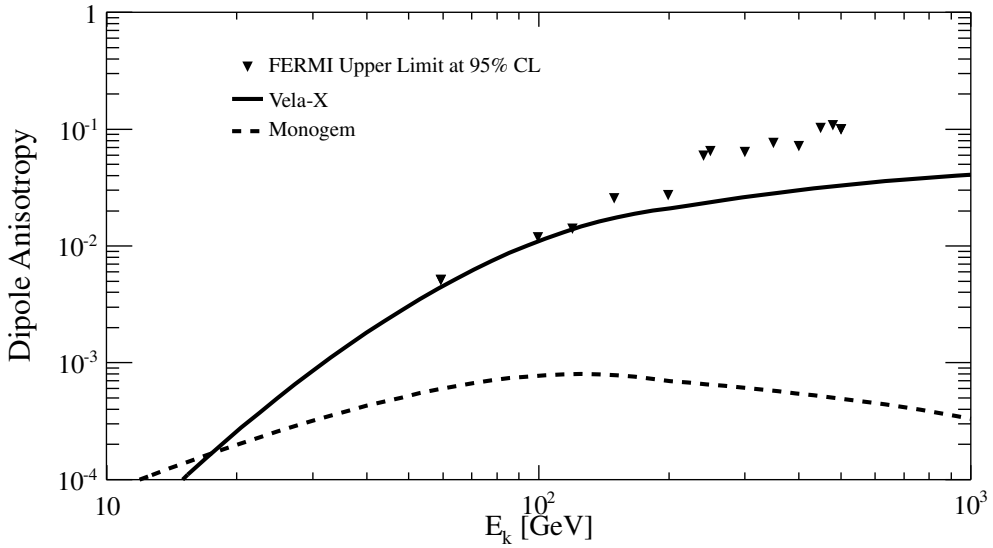

Figure 3: Dipole anisotropy for electron plus positron from Vela-X (solid line) and Monogem (dashed line) compared with the FERMI-LAT upper limits on δ versus the minimum energy for 95% confidence level.

Using the general transport equation (2.1) for a particle density ($N_i = \frac{4\pi}{v_i} I$), where v_i is the particle velocity (see e.g., [21]), the diffusion approximation leads to consider only the first two terms. Under this assumption, the degree of anisotropy from equation (3.2) is:

$$\delta = \frac{I_1}{I_0} = \frac{3F}{4\pi I_0} = \frac{3D_i \left|\vec{\nabla} N_i\right|}{4\pi I_0} = \frac{3}{\beta c} \frac{D_i \left|\vec{\nabla} N_i\right|}{N_i}. \tag{3.4}$$

In our case, equation (3.2) can be rewritten as:

$$\delta = \frac{3D(E)}{\beta c} \frac{2|\vec{x}|}{4\lambda_d^2} \frac{2N_{e^+,source}}{2N_{e^+,source} + N_{e^+,cLIS} + N_{e^-,cLIS}}. \tag{3.5}$$

We remind that the electron and positron spectrum are the sum of a source term and of the cLIS: $N_{e,tot} = N_{e,source} + N_{e,cLIS}$. We assume that particles produced in the ISM, as well as the full positron and electron cLIS, are isotropic; moreover, $N_{e^-,source} = N_{e^+,source}$ because PWN produces these particles in pairs.

The results for our model, described in section 2.2, is reported in figure 3 for both PWN, Vela-X and Monogem in comparison with the most precise available data coming from the FERMI experiment [23] which reports the upper limit at 95% of confidence level for the electron plus positron dipole signal. The analysed dataset corresponds to the first year of LAT science operation and start on August 2008. To minimize the geomagnetic field's influence, the FERMI collaboration has selected ~ 1.6 million events with an energy high enough ($E > 60$ GeV) to elude this effect.

Our model is affected by uncertainties related to the assumption made; in particular the contribution of other sources is not taken into account. However, as shown in figure 3, the degree of anisotropy expected by Vela-X and Monogem, supposed Crab-like at 1000 years, are not excluded by the FERMI data.

PoS(ICRC2015)501

4. Conclusion

In the present work, we have analysed the AMS-02 electron-plus-positron spectrum in the energy range above 10 GeV. A comparison between the AMS-02 data and the cLIS computed with GALPROP shows a discrepancy that can be accounted by adding new astrophysical sources of these particles.

We have evaluated electron and positron spectra generated by PWN and propagated them to the Earth. We supposed that all these objects have the same characteristics at their birth. And we identify these features in the youngest and more studied object, i.e., the Crab Nebula. The model predicts that the main candidates to fit the AMS-02 data are Vela-X, for energy above 100 GeV, and Monogem, for energy below this value. Their contribution, derived from the electron and positron model built to fit the Crab PWN photon data, is in agreement with the AMS-02 flux in the energy range above 10 GeV.

Since only two sources are major contribution to the excess flux, we expect a dipole anisotropy from these objects. The signal expected from Vela-X is $\sim 2\%$ at 200 GeV. The expected anisotropy degree is in the allowed region determined by the FERMI observation.

Acknowledgments

This work is supported by Agenzia Spaziale Italiana under contract ASI-INFN I/002/13/0, Progetto AMS - Missione scientifica ed analisi dati.

References

[1] V. L. Ginzburg and S. I. Syrovatskii, *The Origin of Cosmic Rays*. New York: Macmillan, 1964.

[2] D. Maurin, F. Melot, and R. Taillet, *A database of charged cosmic rays*, *ArXiv e-prints: 1302.5525* (Feb., 2013) [arXiv:1302.5525].

[3] A. Vladimirov, S. Digel, G. JÃşhannesson, P. Michelson, I. Moskalenko, et al., *{GALPROP} webrun: An internet-based service for calculating galactic cosmic ray propagation and associated photon emissions*, *Computer Physics Communications* **182** (2011), no. 5 1156 – 1161.

[4] I. V. Moskalenko and A. W. Strong, *Production and Propagation of Cosmic-Ray Positrons and Electrons*, *The Astrophysical Journal* **493** (1998), no. 2 694.

[5] T. Delahaye, R. Lineros, F. Donato, N. Fornengo, J. Lavalle, P. Salati, and R. Taillet, *Galactic secondary positron flux at the Earth*, *A&A* **501** (July, 2009) 821–833, [arXiv:0809.5268].

[6] S. Della Torre, M. Gervasi, P. Rancoita, D. Rozza, and A. Treves, *Pulsar Wind Nebulae as a source of the observed electron and positron excess at high energy: the case of Vela-X*, *Submitted to JHEAP* (2015).

[7] **AMS-02** Collaboration, M. Aguilar, D. Aisa, B. Alpat, A. Alvino, G. Ambrosi, et al., *Precision Measurement of the $(e^+ + e^-)$ Flux in Primary Cosmic Rays from 0.5 GeV to 1 TeV with the Alpha Magnetic Spectrometer on the International Space Station*, *Phys. Rev. Lett.* **113** (Nov, 2014) 221102.

[8] **AMS-02** Collaboration, M. Aguilar, D. Aisa, A. Alvino, G. Ambrosi, K. Andeen, et al., *Electron and Positron Fluxes in Primary Cosmic Rays Measured with the Alpha Magnetic Spectrometer on the International Space Station*, *Phys. Rev. Lett.* **113** (Sep, 2014) 121102.

PoS(ICRC2015)501

[9] M. J. Rees and J. E. Gunn, *The origin of the magnetic field and relativistic particles in the Crab Nebula*, *Monthly Notices of the RAS* **167** (Apr., 1974) 1–12.

[10] C. F. Kennel and F. V. Coroniti, *Confinement of the Crab pulsar's wind by its supernova remnant*, *Astrophysical Journal* **283** (Aug., 1984) 694–709.

[11] C. F. Kennel and F. V. Coroniti, *Magnetohydrodynamic model of Crab nebula radiation*, *Astrophysical Journal* **283** (Aug., 1984) 710–730.

[12] V. M. Kaspi, M. S. E. Roberts, and A. K. Harding, *Isolated neutron stars*, pp. 279–339. Apr., 2006.

[13] P. Blasi and E. Amato, *Positrons from pulsar winds*, in *High-Energy Emission from Pulsars and their Systems* (D. F. Torres and N. Rea, eds.), p. 624, 2011. arXiv:1007.4745.

[14] D. Malyshev, I. Cholis, and J. Gelfand, *Pulsars versus dark matter interpretation of ATIC/PAMELA*, *Phys. Rev. D* **80** (Sep, 2009) 063005.

[15] F. Aharonian, A. G. Akhperjanian, A. R. Bazer-Bachi, M. Beilicke, W. Benbow, et al., *Observations of the Crab nebula with HESS*, *Astronomy and Astrophysics* **457** (Oct., 2006) 899–915, [astro-ph/0607333].

[16] J. AleksiÄĞ, E. Alvarez, L. Antonelli, P. Antoranz, M. Asensio, et al., *Performance of the {MAGIC} stereo system obtained with crab nebula data*, *Astroparticle Physics* **35** (2012), no. 7 435 – 448.

[17] L. Zhang, S. B. Chen, and J. Fang, *Nonthermal radiation from pulsar wind nebulae*, *The Astrophysical Journal* **676** (2008), no. 2 1210.

[18] S. J. Tanaka and F. Takahara, *A model of the spectral evolution of pulsar wind nebulae*, *The Astrophysical Journal* **715** (2010), no. 2 1248.

[19] J. Martín, D. F. Torres, and N. Rea, *Time-dependent modelling of pulsar wind nebulae: study on the impact of the diffusion-loss approximations*, *Monthly Notices of the RAS* **427** (Nov., 2012) 415–427, [arXiv:1209.0300].

[20] A. A. Abdo, M. Ajello, A. Allafort, L. Baldini, J. Ballet, et al., *The Second Fermi Large Area Telescope Catalog of Gamma-Ray Pulsars*, *The Astrophysical Journal Supplement Series* **208** (2013), no. 2 17.

[21] V. L. Ginzburg and V. S. Ptuskin, *On the origin of cosmic rays: Some problems in high-energy astrophysics*, *Rev. Mod. Phys.* **48** (Apr, 1976) 161–189.

[22] T. Linden and S. Profumo, *Probing the Pulsar Origin of the Anomalous Positron Fraction with AMS-02 and Atmospheric Cherenkov Telescopes*, *The Astrophysical Journal* **772** (2013), no. 1 18.

[23] M. Ackermann, M. Ajello, W. B. Atwood, L. Baldini, J. Ballet, et al., *Searches for cosmic-ray electron anisotropies with the Fermi Large Area Telescope*, *Physical Review D* **82** (Nov., 2010) 092003, [arXiv:1008.5119].

PoS(ICRC2015)501